The ISME Journal (2016) 10, 460–477

www.nature.com/ismej

ORIGINAL ARTICLE

Microorganisms linked to inflammatory bowel disease-associated dysbiosis differentially impact host physiology in gnotobiotic mice

Thomas W Hoffmann[1,2], Hang-Phuong Pham[3], Chantal Bridonneau[1,2], Camille Aubry[1,2], Bruno Lamas[4], Camille Martin-Gallausiaux[1,2], Marco Moroldo[5,6], Dominique Rainteau[4], Nicolas Lapaque[1,2], Adrien Six[7], Mathias L Richard[1,2], Emilie Fargier[8], Marie-Emmanuelle Le Guern[8], Philippe Langella[1,2] and Harry Sokol[1,2,4,6,9]

[1]*INRA, UMR1319 MICALIS, Jouy en Josas, France;* [2]*AgroParisTech, UMR1319 MICALIS, Jouy en Josas, France;* [3]*ILTOO Pharma, Institut du Cerveau et de Moelle Epinière, Hôpital Pitié Salpêtrière, Paris, France;* [4]*ERL INSERM U 1157/UMR7203, Faculté de Médecine Saint-Antoine, Université Pierre et Marie Curie (UPMC), Paris, France;* [5]*INRA, UMR1313 GABI/CRB GADIE, Jouy en Josas, France;* [6]*AgroParisTech, UMR1313 GABI, Jouy en Josas, France;* [7]*Sorbonne Universités, UPMC Université Paris 06, INSERM UMR_S 959, CNRS FRE 3632, Immunology, Immunopathology, Immunotherapy (I3), Paris, France;* [8]*Biocodex, Centre Recherche et Développement, Compiègne, France and* [9]*Service de Gastroentérologie et Nutrition, Hôpital Saint-Antoine, Assistance Publique Hôpitaux de Paris et Université Paris 6, Paris, France*

Studying host–microbiota interactions are fundamental to understanding the mechanisms involved in intestinal homeostasis and inflammation. In this work, we analyzed these interactions in mice that were mono-associated with six microorganisms that are representative of inflammatory bowel disease (IBD)-associated dysbiosis: the bacteria *Bacteroides thetaiotaomicron*, adhesive-invasive *Escherichia coli* (AIEC), *Ruminococcus gnavus* and *Roseburia intestinalis*; a yeast used as a probiotic drug, *Saccharomyces boulardii* CNCM I-745; and another yeast, *Candida albicans*. Extensive *ex vivo* analyses including colon transcriptomics, histology, immune response, bile acid metabolism and short-chain fatty acid production were studied. We showed that *B. thetaiotaomicron* had the highest impact on the immune system because it was almost able to recapitulate the effects of the entire conventional microbiota and notably induced Treg pathways. Furthermore, these analyses uncovered the effects of *E. coli* AIEC LF82 on indoleamine 2,3-dioxygenase expression and of *S. boulardii* CNCM I-745 on angiogenesis. These results were confirmed *in vitro* in human cell lines. Finally, our results suggested that *R. gnavus* has major effects on metabolism, and notably on tryptophan metabolism. This work therefore reveals that microorganisms with a potential role in intestinal homeostasis and inflammation have specific impacts on the host, and it suggests several tracks to follow to understand intestinal homeostasis and IBD pathogenesis better, providing new insights to identify novel therapeutic targets.
The ISME Journal (2016) **10,** 460–477; doi:10.1038/ismej.2015.127; published online 28 July 2015

Introduction

The gastrointestinal tract contains a complex mix of epithelial cells, immune cells, food antigens and microorganisms. The intestinal microbiota is estimated to contain approximately 10^{14} microorganisms, which are primarily bacteria localized in the distal ileum and colon (Ley *et al*., 2006). Although pathogens are rapidly recognized and destroyed by the immune response, the host tolerates the intestinal microbiota by mechanisms that are still unclear (Maynard *et al*., 2012). However, this tolerance can be disrupted and evolve into an uncontrolled inflammatory response (Maynard *et al*., 2012), as observed in pathologies such as inflammatory bowel diseases (IBDs). This deregulation has multiple causes, but dysbiosis (an imbalance in the gut microbiota composition) and genes involved in host–microorganism interactions have been associated with IBD in numerous studies (Sokol *et al*., 2008a; Khor *et al*., 2011), supporting the importance of the microbiota and its interactions with the host in IBD pathogenesis. Studying these interactions is therefore of major interest for understanding the mechanisms involved in IBD in addition to normal gut homeostasis.

Correspondence: H Sokol, Service de Gastroentérologie et Nutrition, Hôpital Saint-Antoine, Assistance Publique Hôpitaux de Paris et Université Paris 6, 184 rue du faubourg Saint-Antoine, 75571, Paris Cedex 12, France.
E-mail: harry.sokol@aphp.fr
Received 6 January 2015; revised 4 June 2015; accepted 16 June 2015; published online 28 July 2015

In this study, we have selected four intestinal bacteria and two yeasts linked to IBD pathogenesis as follows: adhesive-invasive *Escherichia coli* (AIEC), *Ruminococcus gnavus*, *Bacteroides thetaiotaomicron*, *Roseburia intestinalis*, the probiotic yeast *Saccharomyces boulardii* CNCM I-745 and the pathogenic yeast *Candida albicans*. Ileal Crohn's disease (CD) is associated with an increase in *E. coli* and *R. gnavus* representation, in addition to a decrease in *R. intestinalis* representation (Giaffer *et al*., 1991, 1992; Seksik *et al*., 2003; Mangin *et al*., 2004; Willing *et al*., 2010; Joossens *et al*., 2011), the latter being a butyrate producer that is among the most abundant bacteria in human intestinal microbiota (Qin *et al*., 2010). Furthermore, as an original isolate from ileal lesions in a CD patient (Darfeuille-Michaud *et al*., 1998; Boudeau *et al*., 1999), AIEC showed an increased prevalence during this pathology (Darfeuille-Michaud *et al*., 2004) and was reported to worsen the colitis in a mouse model (Carvalho *et al*., 2008). Although contradictory data are available regarding its link to IBD (Sokol *et al*., 2008a), we also chose *B. thetaiotaomicron* because it is a major representative of the *Bacteroidetes* phylum, one of the three major phyla of intestinal microbiota (Qin *et al*., 2010). Finally, the two yeasts were reported as having an impact on intestinal inflammation. On the one hand, *S. boulardii* protects against pathogen-associated diarrhea and colitis in murine models and humans (McFarland *et al*., 1994; Kirchhelle *et al*., 1996; Pothoulakis, 2009), and it reportedly had a beneficial effect on IBD in murine models (Jawhara and Poulain, 2007; Lee *et al*., 2009). On the other hand, *C. albicans* is the most prevalent fungus in human intestinal microbiota and its concentration is increased in IBD patients (Standaert-Vitse *et al*., 2009; Richard *et al*., 2015). Moreover, in the murine colitis model, *C. albicans* worsens intestinal inflammation, and conversely, its colonization is favored by inflammation (Jawhara *et al*., 2008).

These six microorganisms are therefore potential actors in the immune deregulation involved in IBD pathogenesis. The aim of this study was to decipher their effects on the host in murine mono-association models.

Materials and methods

Microorganisms and cell lines

Four bacteria and two yeasts were used in this study as follows: *E. coli* AIEC LF82 (provided by Arlette Darfeuille-Michaud, Clermont Ferrand, France), *R. gnavus* ATCC 29149, *B. thetaiotaomicron* VPI-5482 (ATCC 29148), *R. intestinalis* L1-82 (DSM 14610), *S. boulardii* CNCM I-745 (syn. HANSEN CBS 5926, Biocodex Laboratories, Gentilly, France) and *C. albicans* SC5314 (ATCC, Molsheim, France). HT-29 (human colon epithelium; ATCC) and HUVEC (human umbilical vein endothelium; Lonza, Levallois-Perret, France) cell lines were also used for *in vitro* experiments. The growth and culture conditions are described in Supplementary Information.

Mono-associations

All procedures were carried out according to European guidelines for the care and the use of laboratory animals. Animal experiments were evaluated and approved by the local ethics committee. Germ-free female C3H/HeN mice (ANAXEM platform, INRA, France) were bred in germ-free isolators. Bacterial suspensions (10^8–10^9 colony forming unit (CFU) in 400 µl), yeast suspensions (10^7–10^8 CFU in 400 µl), or control medium was administered to 6-week-old mice by intragastric gavage (eight mice per group).

For conventionalization, fresh stools from C3H/HeN mice were immediately transferred to an anaerobic chamber, in which the stools were suspended and diluted 1:100 in LYHBHI medium (BD Difco, Le Pont de Claix, France) supplemented with cellobiose (1 mg ml^{-1}; Sigma-Aldrich, Saint Quentin Fallavier, France), maltose (1 mg ml^{-1}; Sigma-Aldrich) and cysteine (0.5 mg ml^{-1}; Sigma-Aldrich). Six-week-old germ-free mice were inoculated by oral gavage with 400 µl of fecal suspension.

After 6 weeks of implantation, the mice were killed and several samples were taken, namely the pieces and content from the jejunum, ileum, cecum and colon, and mesenteric lymph nodes (MLNs).

The microorganism population levels were determined in the feces during implantation (weekly) and in the intestinal contents after killing, all with culture methods (LYHBHI-agar or Sabouraud-agar).

SCFA and bile acid analysis

A measurement of the short-chain fatty acids (SCFAs) was performed on the cecal contents by gas chromatography coupled with mass spectrometry, according to a previously described procedure (Ferchaud-Roucher *et al*., 2005). D3-acetate, D5-propionate and 13C-butyrate (Sigma-Aldrich) were used as internal standards. The selected ion monitoring mode was used to measure SCFA concentrations with ions at m/z 117 (acetate), 120 (D3-acetate), 131 (propionate), 136 (D5-propionate), 145 (butyrate) and 146 (13C-butyrate).

The bile acid composition and concentration were measured in feces at 6 weeks post-gavage by high-performance liquid chromatography coupled to tandem mass spectrometry, as previously described (Humbert *et al*., 2012).

Histology

Colon samples for histological studies were fixed in 4% paraformaldehyde acid (Electron Microscopy Sciences, Hatfield, PA, USA), embedded in paraffin, then stained for histological scoring and immunohistochemistry analysis, as described in Supplementary Information.

The quantification of cytokines and immunoglobulins
The MLNs were mashed with a 70-μm cell strainer in cell culture medium, and 2.10^5 cells per well were cultured in P24 plates for 48 h (37 °C, 10% CO_2) with stimulation by anti-CD3/CD28 antibodies (4 μg ml^{-1} each; eBioscience, Paris, France) or phorbol 12-myristate 13-acetate/ionomycin (50 ng ml^{-1} and 1 μM, respectively; Sigma-Aldrich). For the IgA quantification, the feces were homogenized in phosphate-buffered saline (1 ml per 100 mg) and centrifuged. All collected supernatants were frozen at −80 °C until processing. The quantification of mouse cytokines or immunoglobulins was performed by enzyme-linked immunosorbent assay (ELISA), according to the manufacturer's instructions with interleukin-4 (IL-4), IL-5, interferon-γ (IFNγ), IL-17, IL-10 and IgA (MabTech, Nacka Strand, Sweden); and transforming growth factor-β (TGFβ) and IL-22 (DuoSet ELISA Development System, R&D Systems, Lille, France).

Gene expression
The total RNA was isolated from colon samples and cell lines with an RNeasy Mini Kit (Qiagen, Courtaboeuf, France), according to the manufacturer's instructions. The RNA integrity was checked on a Bioanalyzer 2100 by using RNA 6000 Nano chips (Agilent Technologies, Les Ulis, France), and all the samples had a RNA integrity number score higher than 8.

Transcriptional profiling was performed on the mouse colon samples by using the SurePrint G3 Mouse GE 8×60K Microarray (Design ID: 028005, Agilent Technologies), as described in Supplementary Information. The microarray data were submitted to GEO (accession number: GSE63299). In addition, the expression of selected mouse and human genes was assessed in mouse colon and human cells by reverse transcriptase (RT)-quantitative PCR (qPCR), as described in Supplementary Information.

In vitro experiments
HT-29-IDO reporter cells were generated and used to monitor the effect of *E. coli* LF82 on IDO-1 transcription activity, as well as the HUVEC cell line was used to test the vascular effects of *S. boulardii*. Detailed protocols are described in Supplementary Information.

Data analysis and statistics
Transcriptomic data obtained from microarrays were analyzed as described in Supplementary Information. For all the data in the graphs, the results were expressed as the mean or mean ± s.e.m. ($n = 3$ to 8 per group). Kruskal–Wallis test was used for multiple comparisons, and Mann–Whitney test with Bonferroni correction for 2–2 group comparison.

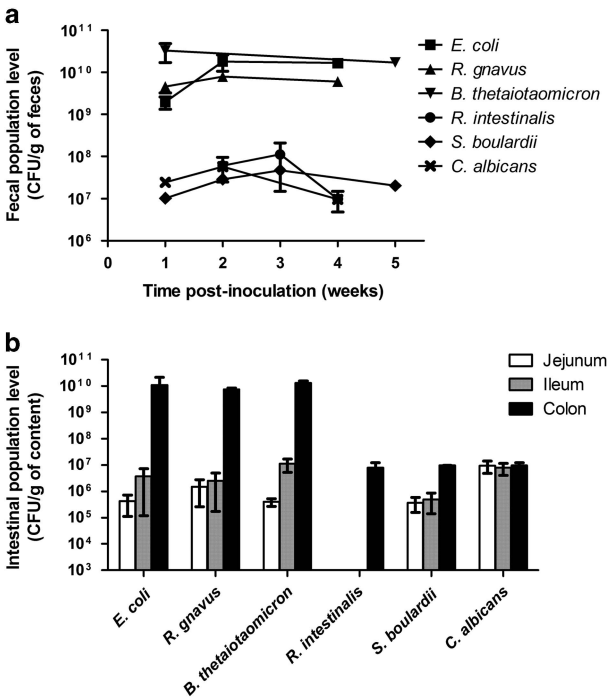

Figure 1 Microbial population levels in mono-associated mice. Population levels were determined in feces during implantation (**a**) and in different intestinal contents after killing (**b**) using culture methods on LYHBHI-agar or Sabouraud-agar. Results are expressed as mean ± s.e.m. ($n = 8$ per group).

Results

Microbial implantation and the metabolic and morphological effects of mono-associations
Six mono-association models involving four bacteria in addition to probiotic yeast and pathogenic yeast, all of which were linked to IBD pathogenesis, were studied. All the microorganisms rapidly and stably colonized the guts of germ-free mice as evidenced by the feces quantifications (Figure 1a). However, two distinct patterns were observed (Figure 1a) as follows: *E. coli*, *R. gnavus* and *B. thetaiotaomicron* reached high population levels (10^{10}–10^{11} CFU per g of feces), and the population levels of *R. intestinalis*, *S. boulardii* and *C. albicans* were lower (10^7–10^8 CFU per g of feces). The population levels in the colon contents confirmed these results (Figure 1b). Strikingly, *E. coli*, *R. gnavus* and *B. thetaiotaomicron* but not the two yeasts presented a markedly decreased level in the small intestine (the jejunum and ileum) when compared with the colon. This finding suggests fitness differences between microorganisms with the bacteria being more adapted to the colon environment and fungi being equally adapted to the small and large intestines. *R. intestinalis* poorly colonized only the colon, suggesting a higher growth requirement (Figure 1b).

Gut bacteria have high metabolic activity and metabolites that deeply impact the host's physiology. Among these metabolites, SCFA production and bile acid metabolism are among the most important.

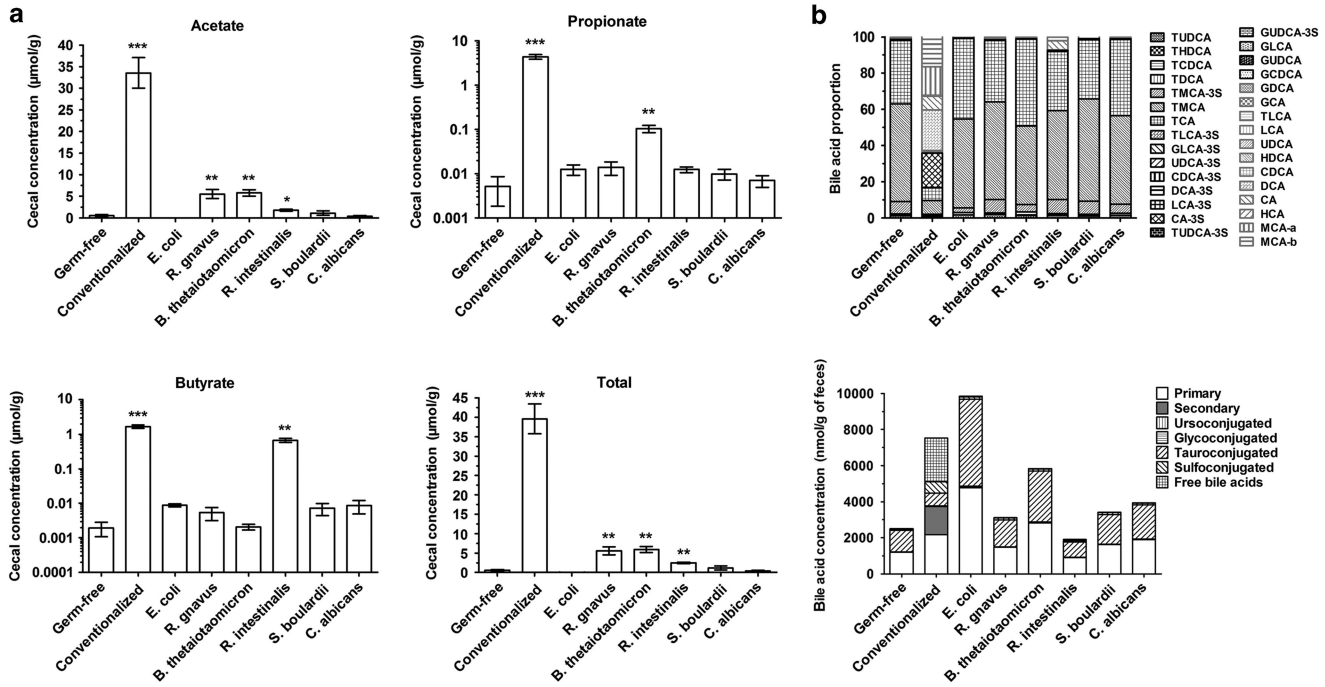

Figure 2 Cecal concentration of SCFAs and fecal level of bile acids in mono-associated mice. (**a**) Acetate, propionate and butyrate concentration were determined in cecal content by gas chromatography coupled with mass spectrometry. Results are expressed as mean ± s.e.m. ($n = 5$ per group). Statistical comparison with the germ-free group was performed using Mann–Whitney *U*-test (*$P < 0.05$/ **$P < 0.01$/***$P < 0.001$). (**b**) Bile acid composition was measured in feces at 6 weeks post-gavage by high-performance liquid chromatography coupled to tandem mass spectrometry, and was represented here with the concentration of bile acid families or individual bile acid proportion. Results are expressed as mean of five mice per group.

To gain insight into bacterial metabolism, we thus determined the SCFA and bile acid concentrations in the cecal and fecal contents, respectively. In comparison with germ-free mice, the global SCFA concentration was significantly increased in mice colonized with *B. thetaiotaomicron*, *R. gnavus* and *R. intestinalis* but did not reach the level observed in conventionalized mice (Figure 2a). We observed that the butyrate production by *R. intestinalis* was similar to that of conventionalized mice, there was moderate acetate production by *B. thetaiotaomicron* and *R. gnavus*, and there was moderate propionate production by *B. thetaiotaomicron* (Figure 2a).

With regard to the bile acid composition in the stool, major differences were observed between germ-free and conventionalized mice as expected, the most important being the appearance of secondary bile acids (Figure 2b and Supplementary Figure 1). However, mono-associated mice exhibited only minor differences in comparison with germ-free mice (Figure 2b). Although the global bile acid concentration was higher in mice that were mono-colonized with some bacteria (*E. coli* and *B. thetaiotaomicron*) in comparison with germ-free mice, no secondary bile acid was detected (Figure 2b). This finding shows that none of the tested microorganisms was able to deconjugate primary bile acids efficiently. Similar results were also observed in a context of simplified microbiota with different cocktails of the tested microorganisms (data not shown), indicating that major actors of primary bile acid deconjugation are lacking.

Finally, the colon histology results were compared between our different models. We observed an increase in the crypt depth and goblet cell density in mono-associated groups in comparison with germ-free mice, as observed in conventionalized mice (Supplementary Figure 2). Strikingly, *S. boulardii* was the only microorganism that did not induce an increase in the crypt depth (Supplementary Figure 2A). The colon epithelial cell proliferation assessed by the height of Ki67 staining in the crypts showed that *B. thetaiotaomicron* decreased this proliferation whereas *R. intestinalis* increased proliferation (Supplementary Figure 2C). As expected, conventionalized mice showed the highest proliferation level.

Host transcriptomics reveal distinct profiles for several mono-associations

Total RNA was extracted from colon tissues and analyzed by microarrays to determine host transcriptomic profiles. A principal component analysis showed that germ-free and conventionalized mice had markedly different profiles, confirming that the gut microbiota has a major impact on host gene expression. Different types of global expression profiles were observed in mono-colonized mice (Figure 3a). *E. coli* and *R. gnavus* induced profiles

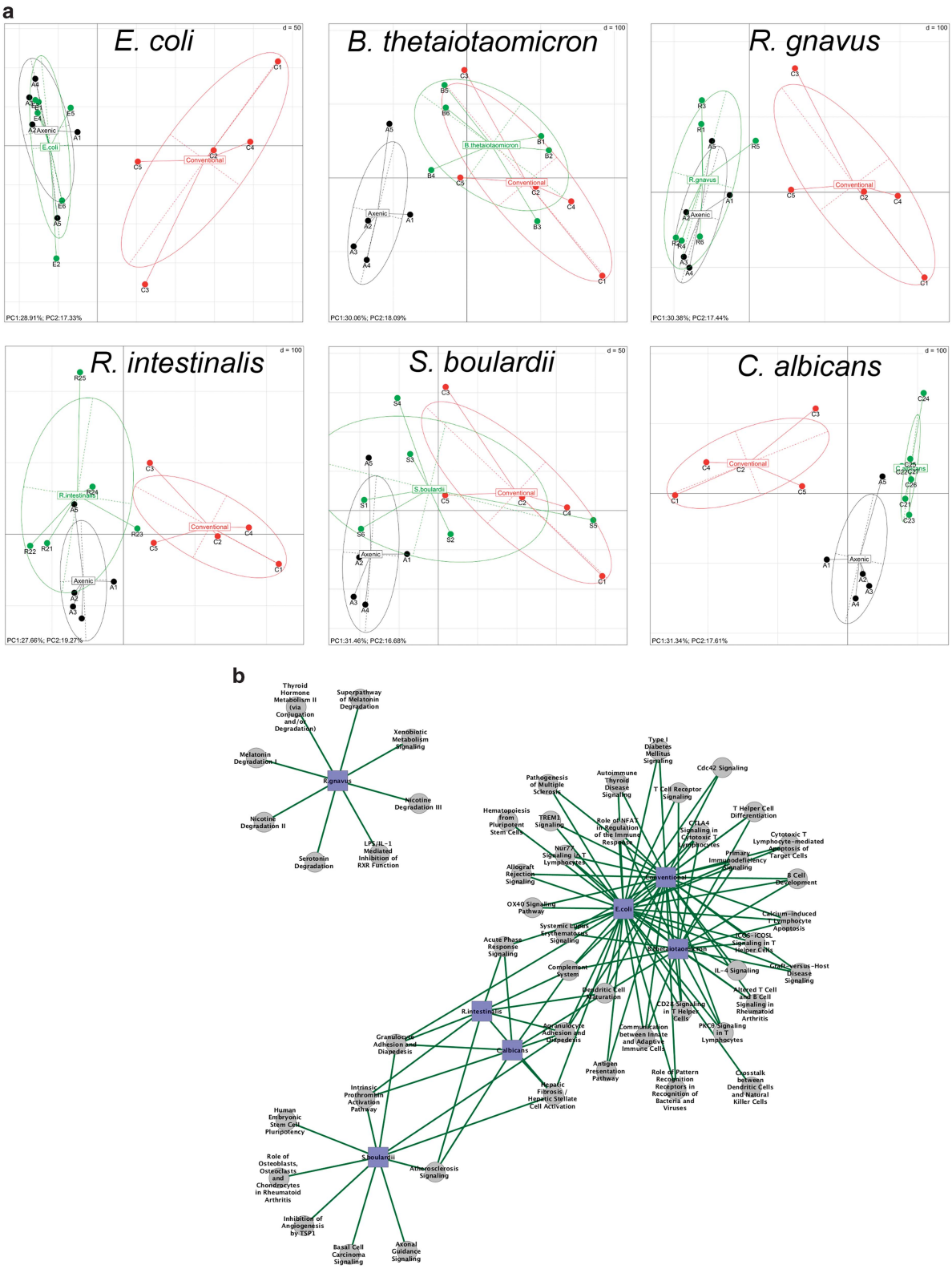

Figure 3 Colon gene expression in mono-associated mice using microarray technology. (**a**) Gene expression in mouse colon was analyzed by principal component analysis. The ellipses delimit mono-associated group (monoxenic, in green), germ-free group (axenic, in black) and conventionalized group (conventional, in red). The axes correspond to principal component 1 (x axis) and 2 (y axis). (**b**) Interaction network established with Cytoscape and showing nodes and connections between significantly enriched ingenuity canonical pathways, in each mono-associated group when compared with germ-free mice. The gray circle nodes represent the ingenuity canonical pathways and the blue square nodes represent the mono-associated group compared with germ-free mice. The green edge links represent significantly upregulated functions/pathways in mono-associated groups compared to germ-free group. Significant level was fixed at $\alpha = 0.05$.

similar to those of germ-free mice, and *R. intestinalis* and *S. boulardii* induced profiles that were intermediate between germ-free and conventionalized mice, whereas *C. albicans* induced a profile that was totally distinct from those of the control groups. Surprisingly, a mono-association with *B. thetaiotaomicron* was sufficient to induce an expression profile similar to that of conventionalized mice.

As expected, an analysis of modulated genes and signatures in comparison with germ-free mice showed the high dominance of immune response features (Supplementary Figures 3 and 4, Table 1). This finding was especially clear for the *B. thetaiotaomicron* model, which shared the highest number of deregulated pathways with conventionalized mice (Figure 3b), and occasionally similar deregulation levels in signature and gene expression levels (Supplementary Figures 3 and 4). Furthermore, the *B. thetaiotaomicron* model was the only one with a lack of immune response-related pathways in the top downregulated signature when compared with conventionalized mice, rather showing deregulation in DNA and cell

Table 1 Selection of significant upregulated genes when compared with germ-free mice

Implantation	*Genes*	*Fold change*	*Description*
Conventionalized	Igj	468.0	Ig chain linker
	Trpv6	18.8	Calcium channel
	Ly6e	13.7	Proliferation of lymphocytes
	Reg3b	12.0	Antimicrobial peptide
	Ifi27l2a/Ifi47/Ifi44	11.9/8.3/6.1	IFN-induced factors
	Ccl5	8.6	Chemokine
	Cd3d/Cd3g	7.1/5.8	CD3 chains
	H2-DMb1/H2-Aa/H2-Ab1/H2-DMa	7.1/7.0/6.4/5.9	CMH II
B. thetaiotaomicron	Igj	207.0	Ig chain linker
	C1s	5.1	Complement subunit
	Cd3d/Cd3g	4.3/3.4	CD3 chains
	Ifitm1	4.2	IFN-induced factor
	Mcpt4/Mcpt2/Mcpt1	4.2/4.0/3.8	Mast cell proteases
	Trem2	3.6	Inflammatory receptor
	Ccl5	3.5	Chemokine
E. coli	Igj	96.7	Ig chain linker
	Reg3b/Reg3g	63.3/12.9	Antimicrobial peptides
	S100g/Slc10a2	11.5/5.4	Solute transporters
	Mmp7	7.2	Matrix metalloproteinase
	Ifi47	4.7	IFN-induced factor
	Ido1	4.5	Tryptophan metabolism
	Tlr13	4.4	Pattern recognition receptor
	Cxcl9	3.8	Chemokine
R. gnavus	Igj	33.0	Ig chain linker
	Cyp3a44/3c55/3a16/3a59	7.5/5.9/5.2/3.1	Cytochrome P450 members
	Reg1	3.8	Antimicrobial peptide
	Tlr13	3.7	Pattern recognition receptor
	Ido1	3.0	Tryptophan metabolism
R. intestinalis	Igj	8.1	Ig chain linker
	Dbp/Tef	7.4/3.1	Circadian rhythm
	C1s	5.1	Complement subunit
	S100g/Slc2a5/Slc10a2	5.0/4.0/3.8	Solute transporters
	Trem2	3.6	Inflammatory receptor
	Cxcl12	3.5	Chemokine
	Mcpt4	3.3	Mast cell protease
	Esm1/Egfl7	3.3/3.3	Produced by endothelial cells
	Clec3b	3.2	Pattern recognition receptor
S. boulardii	Tex14	6.3	Cell division
	C1s	5.2	Complement subunit
	Igj	4.5	Ig chain linker
	Esm1/Egfl7/Glycam1/Apln	4.4/3.3/3.1/1.9	Produced by endothelial cells
	Mcpt4	3.0	Mast cell protease
	Col1a2/18a1	1.8/1.6	Collagen subunits, linked to angiogenesis
C. albicans	Igj	9.5	Ig chain linker
	Esm1	5.3	Produced by endothelial cells
	Trpv6	4.7	Calcium channel
	Mcpt4	4.7	Mast cell protease
	Col6a3/1a2/5a1/5a3/6a1	4.0/3.9/3.9/3.4/3.2	Collagen subunits
	Cd93	3.8	C-type lectin receptor on immune and endothelial cells
	Cxcl12	3.3	Chemokine
	Clec3b	3.3	Pattern recognition receptor

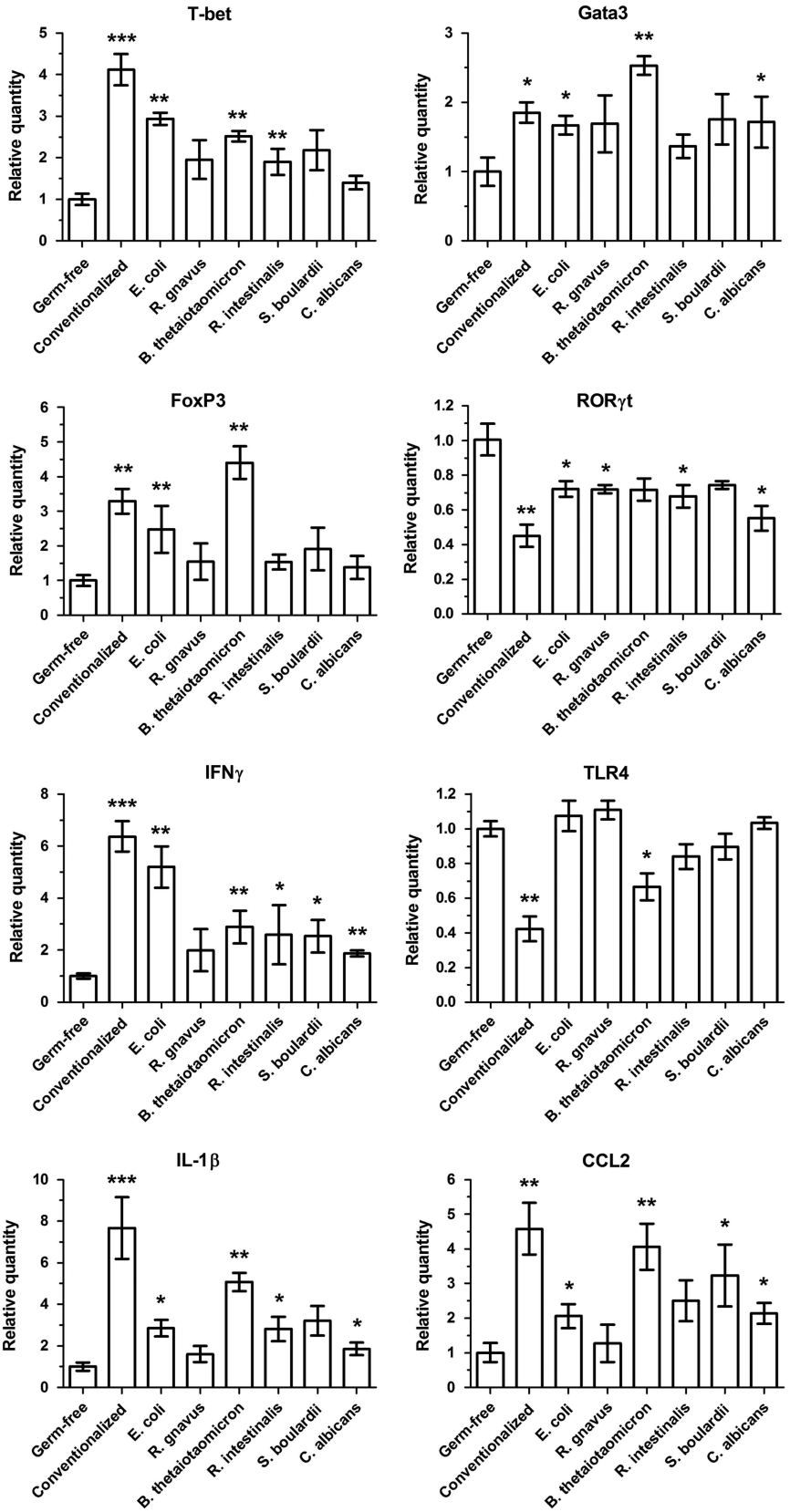

Figure 4 Colon immune gene expression in mono-associated mice. To confirm results from microarrays, the genes of eight immune proteins were selected and their RNA expression was determined in colon by RT-qPCR. The ΔΔCt method was used for quantification, with GAPDH as an internal control and germ-free group as a calibrator. Results are expressed as mean ± s.e.m. ($n = 5$ per group). Statistical comparison with the germ-free group was performed using Mann–Whitney *U*-test (*$P<0.05$/**$P<0.01$/***$P<0.001$).

division processes (Supplementary Figures 5 and 6, Supplementary Table 2). This finding suggests that *B. thetaiotaomicron* by itself is able to induce an immune system maturation that is close to the one induced by conventionalization.

Strikingly, when compared with germ-free mice, some mono-association models presented top expression signatures that were not related to the immune response. In fact, the top upregulated signature in the *R. gnavus* model contained only metabolic pathways, and the top upregulated signature of the *S. boulardii* model contained only pathways related to vascular processes and endothelial cells with genes harboring pro- or anti-angiogenic activity (Figure 3b).

In addition, a comparison of the gene expression with germ-free mice confirmed the metabolic profile induced by *R. gnavus* with the upregulation of several cytochrome P genes, in addition to the vascular profile induced by *S. boulardii* with the upregulation of several endothelial genes and genes involved in pro- or anti-angiogenic processes (Table 1). Strikingly, the indoleamine 2,3-dioxygenase gene (Ido1) was particularly upregulated in the colon from *E. coli* LF82 mono-associated mice (Table 1), but no significant increase was observed in other models or controls except for *R. gnavus*.

Based on the host transcriptomic profiles, we selected three interesting features for further analysis as follows: (i) *B. thetaiotaomicron* and the high maturation of the colon immune system; (ii) *E. coli* LF82 and Ido1 gene induction; and (iii) *S. boulardii* and the induction of endothelial pathways.

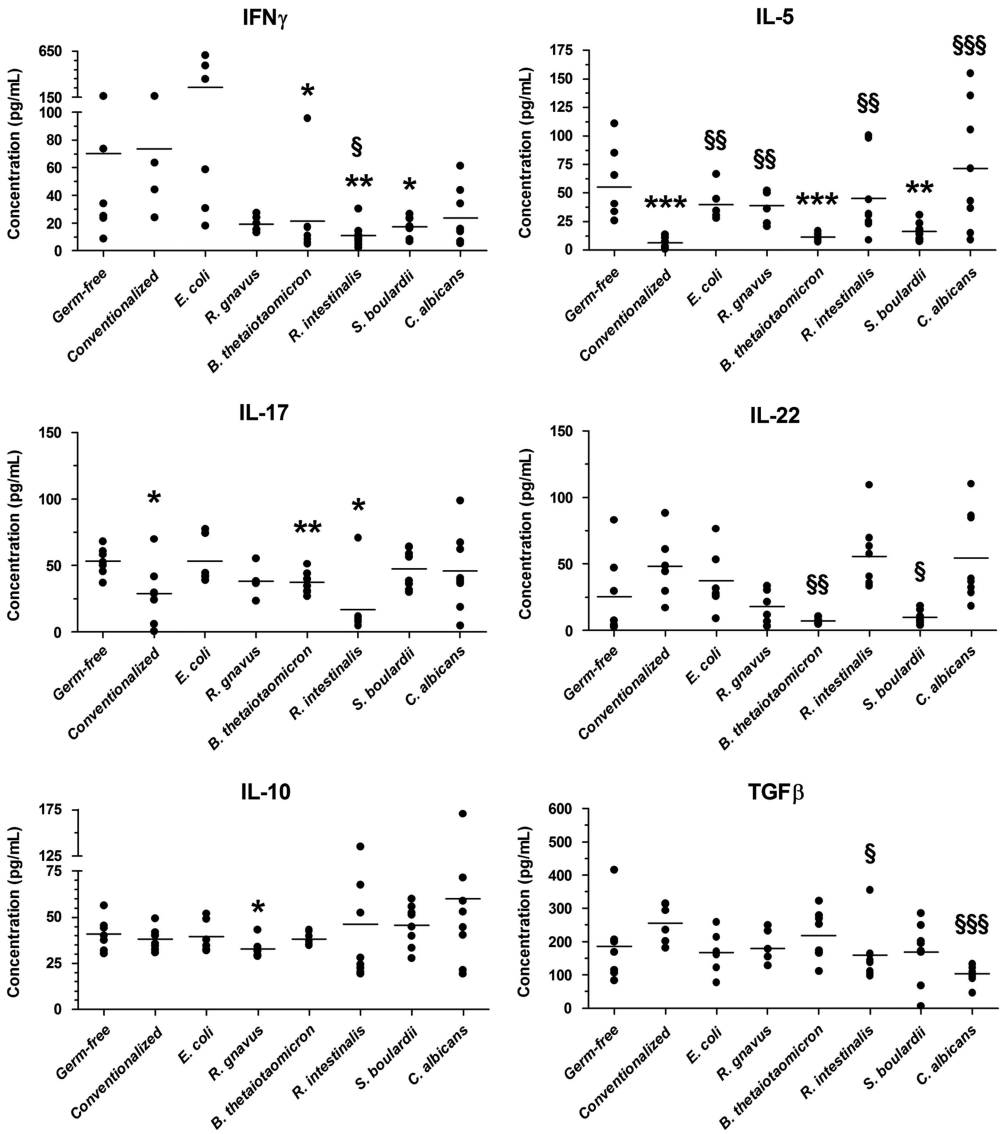

Figure 5 Cytokine production in MLNs from mono-associated mice. Cells were isolated from MLNs and cultured for 48 h with anti-CD3/CD28 antibodies to activate them. ELISA was performed on supernatants to quantify the production of six cytokines representative of major T-helper cytokine profiles. The mean value for each experimental group is indicated by a horizontal bar ($n = 8$ per group). Statistical comparison with the germ-free group ($^{*}P<0.05/^{**}P<0.01/^{***}P<0.001$) and with conventionalized mice ($^{\S}P<0.05/^{\S\S}P<0.01/^{\S\S\S}P<0.001$) was performed using Mann–Whitney *U*-test.

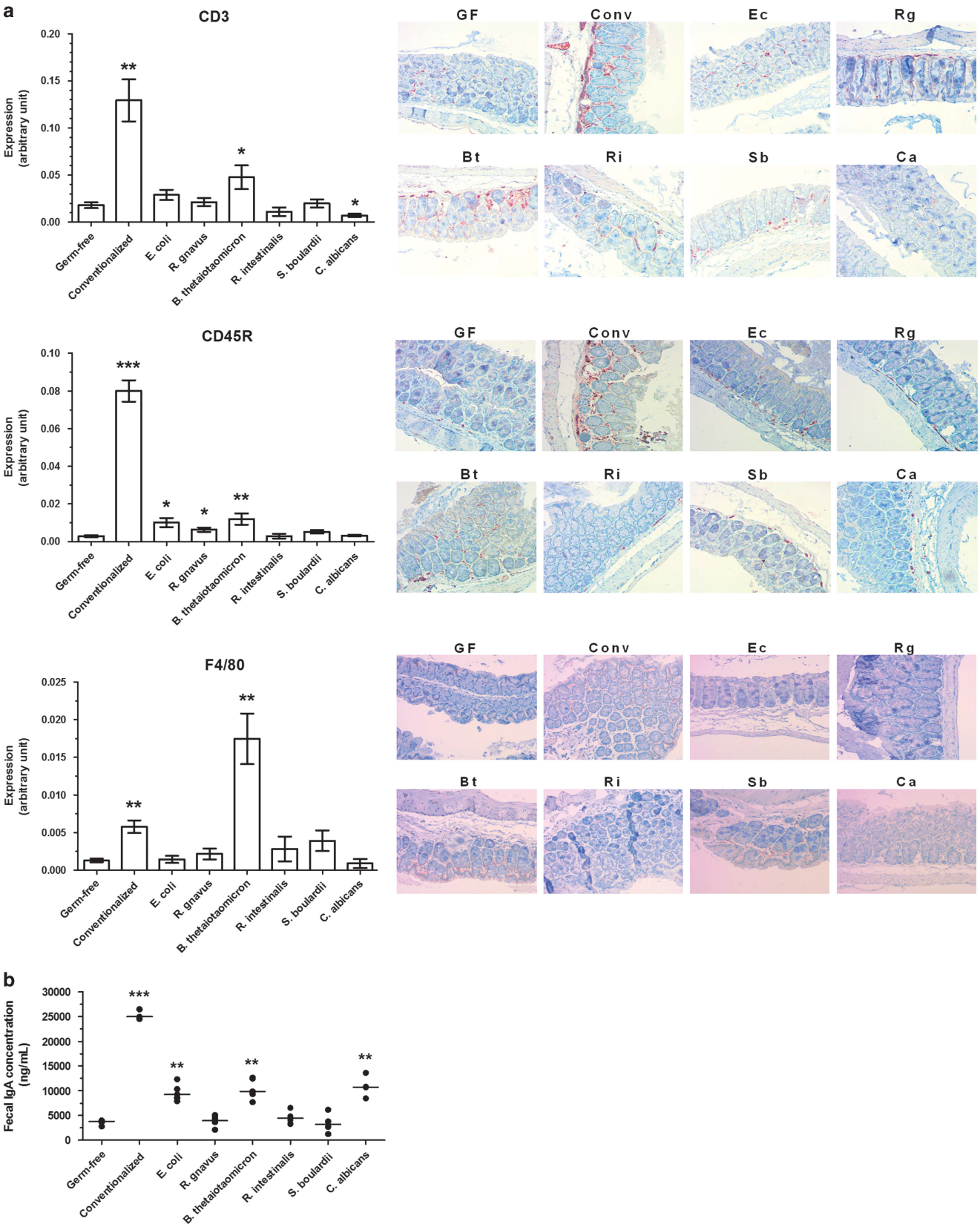
a
CD3
Expression (arbitrary unit)
0.20
0.15
0.10
0.05
0.00
**
*
*
Germ-free
Conventionalized
E. coli
R. gnavus
B. thetaiotaomicron
R. intestinalis
S. boulardii
C. albicans
GF
Conv
Ec
Rg
Bt
Ri
Sb
Ca
CD45R
Expression (arbitrary unit)
0.10
0.08
0.06
0.04
0.02
0.00
***
*
*
**
F4/80
Expression (arbitrary unit)
0.025
0.020
0.015
0.010
0.005
0.000
**
**
b
Fecal IgA concentration (ng/mL)
30000
25000
20000
15000
10000
5000
0
***
**
**
**

Bacteroides thetaiotaomicron strongly induces the maturation of the colon immune system including Treg pathway activation

We confirmed the immune response gene deregulation observed in the microarrays in the different models by using RT-qPCR to target major T-cell transcription factors and other selected genes (Figure 4). Consistent with the microarray data, the RT-qPCR results for the *B. thetaiotaomicron* model were often similar to those found in conventionalized mice (Figure 4). Strikingly, when compared with germ-free mice, this model showed a strong increase in Gata3 and FoxP3 gene expression, even higher than in conventionalized mice (Figure 4).

The production of representative cytokines from the major T-helper profiles were quantified in MLNs after stimulation by anti-CD3/CD28 antibodies. For most cytokines, only modest differences were observed between the groups (Figure 5). *B. thetaiotaomicron* induced a slight but significant reduction in Th1, Th2 and Th17 cytokines (Figure 5). We also observed that *R. intestinalis* induced decreased IFNγ and IL-17 production with increased IL-22 production, corresponding to an anti-inflammatory pattern. *S. boulardii* induced decreased IFNγ and IL-5 production (Figure 5). Global stimulation with phorbol 12-myristate 13-acetate/ionomycin showed similar results for *B. thetaiotaomicron*, *R. intestinalis* and *S. boulardii*, but *R. gnavus* and *C. albicans* showed a pro-inflammatory profile with increased IFNγ, IL-17 and IL-22 production (Supplementary Figure 7).

We then explored the local induction of immunity by *B. thetaiotaomicron*. T cells, B cells and macrophages were quantified in the colon by immunohistochemistry (by using anti-CD3, anti-CD45R and anti-F4/80 antibodies, respectively). In comparison with germ-free mice, only *B. thetaiotaomicron* increased the presence of these three immune cell types (Figure 6a). *B. thetaiotaomicron* also induced an IgA increase in the feces (which represents mucosal immunity and, notably, gut plasma cell responses), in addition to *E. coli* and *C. albicans* (Figure 6b). Consistent with the MLNs results, *R. intestinalis* and *S. boulardii* increased neither the number of immune cells in the colon nor the IgA level in the feces (Figures 6a and b).

As Foxp3 expression was markedly increased in the colon of *B. thetaiotaomicron*-colonized mice (RT-qPCR results, Figure 4), we explored the induction of Treg pathways by this bacterium. As observed in Figure 7a, many genes involved in Treg pathways and functions were upregulated by *B. thetaiotaomicron* in comparison with germ-free mice and other mono-colonized mice, often at the same level as those of conventionalized mice. Three major genes involved in Treg pathways (IL-10, TGFβ and PDCD1) were selected, and we confirmed the upregulation of these three genes by *B. thetaiotaomicron* (but not by other bacteria) with RT-qPCR (Figure 7b). Finally, Treg cells in colon samples were stained by immunohistochemistry with anti-FoxP3 antibodies, and the induction of Treg cells by *B. thetaiotaomicron* was confirmed, whereas other bacteria presented low induction (Figure 7c).

Escherichia coli LF82 induces IDO gene expression in the colon

To confirm the microarray results with *E. coli* LF82, Ido1 expression was tested by RT-qPCR in colon samples. This gene was strongly induced in *E. coli* LF82 mono-associated mice when compared with germ-free mice and its expression was not modified in conventionalized mice or in other mono-associations except for *R. gnavus* (Figure 8a). We then tested IDO gene expression in humans using an HT-29 colon epithelial cell line with a luciferase reporter system. The IDO gene was induced by an *E. coli* LF82 supernatant or pellet, but it was not induced by the non-CD-associated *E. coli* MG1655 strain or by the *R. gnavus* strain used in our mono-association study (Figure 8b). However, this induction was lower than it was with the common IDO inducers IFNγ and IL-1β (Figure 8b). As *R. gnavus* mono-associated mice presented Ido1 upregulation in the colon and this increase was not observed in the luciferase reporter epithelial cell system, it suggests a possible effect on other cell types such as dendritic cells or an indirect effect via IDO-activating cytokines (such as type I or type II IFN).

S. boulardii stimulates endothelial gene expression and matures blood vessels in the colon

Two of the endothelial genes upregulated by *S. boulardii* in colon microarrays, namely Esm1 and Egfl7, were selected and their expression was tested by RT-qPCR in colon samples. These genes are involved in angiogenesis stimulation and are upregulated during angiogenesis (Nichol and Stuhlmann, 2012; Rocha *et al*., 2014). The upregulation of these two genes was confirmed, with expression higher than that in conventionalized mice (Figure 9a). We then wanted to confirm this endothelial effect at the morphological level in mice.

Figure 6 Colon immunity in mono-associated mice. (**a**) Colon samples were fixed in paraformaldehyde acid, embedded in paraffin and sliced in 4-μm sections, then stained by immunohistochemistry with rabbit polyclonal anti-CD3 antibody (T cells), rat monoclonal anti-CD45R antibody (B cells) and rat monoclonal anti-F4/80 antibody (macrophages). (**b**) IgA production was determined by ELISA in feces at 6 weeks post-gavage. In graphs, results are expressed as mean ± s.e.m. ($n = 5$ per group) and statistical comparison with the germ-free group was performed using Mann–Whitney *U*-test (*$P<0.05$/**$P<0.01$/***$P<0.001$). Representative photos were taken with x100 magnification. Bt, *B. thetaiotaomicron*; Ca, *C. albicans*; Conv, conventionalized; Ec, *E. coli*; GF, germ-free; Rg, *R. gnavus*; Ri, *R. intestinalis*; Sb, *S. boulardii*.

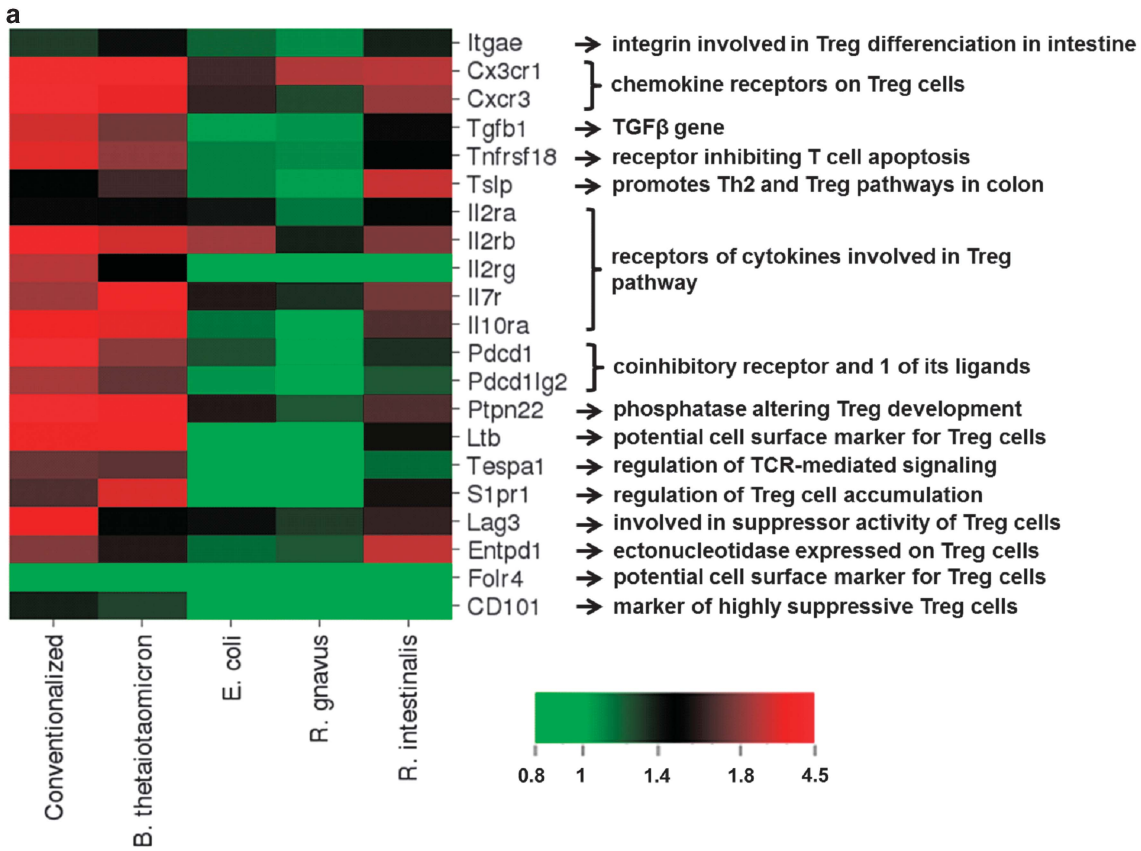
a
Itgae
Cx3cr1
Cxcr3
Tgfb1
Tnfrsf18
Tslp
Il2ra
Il2rb
Il2rg
Il7r
Il10ra
Pdcd1
Pdcd1lg2
Ptpn22
Ltb
Tespa1
S1pr1
Lag3
Entpd1
Folr4
CD101
integrin involved in Treg differenciation in intestine
chemokine receptors on Treg cells
TGFβ gene
receptor inhibiting T cell apoptosis
promotes Th2 and Treg pathways in colon
receptors of cytokines involved in Treg pathway
coinhibitory receptor and 1 of its ligands
phosphatase altering Treg development
potential cell surface marker for Treg cells
regulation of TCR-mediated signaling
regulation of Treg cell accumulation
involved in suppressor activity of Treg cells
ectonucleotidase expressed on Treg cells
potential cell surface marker for Treg cells
marker of highly suppressive Treg cells
Conventionalized
B. thetaiotaomicron
E. coli
R. gnavus
R. intestinalis
0.8
1
1.4
1.8
4.5

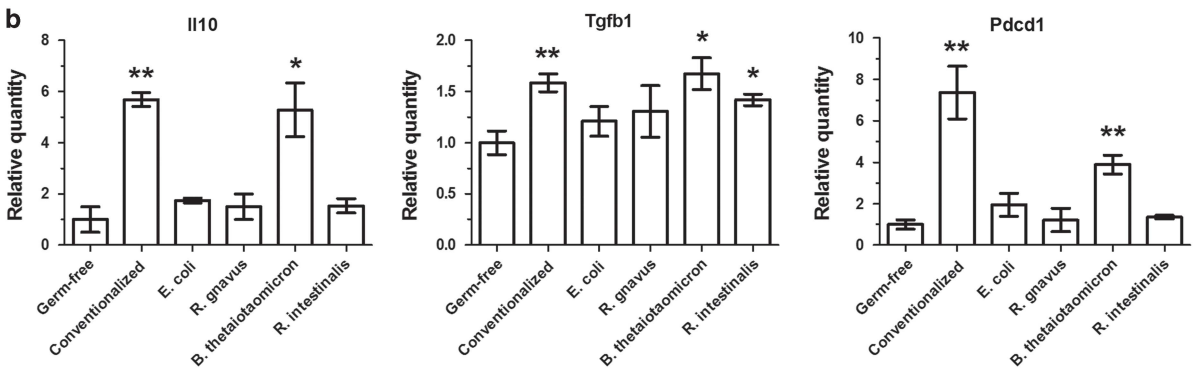
b
Il10
Tgfb1
Pdcd1
Relative quantity
Germ-free
Conventionalized
E. coli
R. gnavus
B. thetaiotaomicron
R. intestinalis

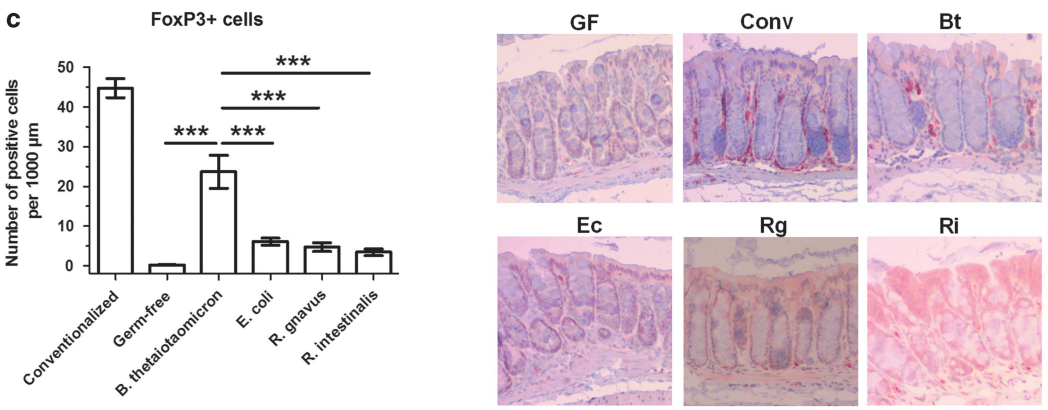
c
FoxP3+ cells
Number of positive cells per 1000 µm
GF
Conv
Bt
Ec
Rg
Ri

To confirm these observations, endothelial cells were stained by immunohistochemistry (anti-CD31 antibody) and the vessels were analyzed in the colon. In comparison with germ-free mice, *S. boulardii* promoted a twofold increase in the blood vessel diameter, at a level similar to that of conventionalized mice (Figures 9b and c). A trend was observed with regards to an increase in the blood vessel number (Supplementary Figure 8). The *S. boulardii* mono-associated model was the only one to exhibit a profile of vessel diameters similar to that of conventionalized mice, whereas other mono-colonized mice models were more similar to germ-free mice or intermediate between conventionalized and germ-free mice (Figure 9c and Supplementary Figure 8).

To assess the effect of *S. boulardii* on vessels directly, a human endothelial cell line (HUVEC) was stimulated with *S. boulardii* culture supernatant and the expression of Esm1, CD36, Vegfr2 and Tie2 was assessed. These genes are involved in pro-angiogenic (Esm1, Vegfr2 and Tie2) or anti-angiogenic (CD36) processes (Febbraio *et al.*, 2001; Roskoski, 2008; Cascone and Heymach, 2012; Rocha *et al.*, 2014), and they were upregulated and/or present in the top upregulated expression signature as shown by the microarray assays performed on *S. boulardii* mono-colonized mice. We observed that *S. boulardii* culture supernatant induced the expression of the four endothelial genes, when compared with the control medium (Figure 9d), confirming the modulation of angiogenesis and the maturation of blood vessels by the yeast.

Discussion

Gut microbiota–host crosstalk is crucial for intestinal homeostasis in addition to the pathogenesis of diseases such as IBD. In this study, we selected four bacteria in addition to a probiotic yeast and a pathogenic yeast, all of which are representative of intestinal microbiota and/or are linked to IBD (and are therefore considered potential actors in the immune deregulation associated with these diseases), and we studied their impacts on the host in the context of mono-association. Although a decrease in *Faecalibacterium prausnitzii* was reported as a key factor in CD pathogenesis (Sokol *et al.*, 2008b), this bacterium was not selected for study because we were not able to establish mono-associated mice with it. Some of these microorganisms were previously used for mono-association in rodents, such as *B. thetaiotaomicron* (Hooper *et al.*, 2001; Lecuit *et al.*, 2007; Wrzosek *et al.*, 2013; Perez-Munoz *et al.*, 2014), *S. boulardii* (Rodrigues *et al.*, 1996; Martins *et al.*, 2009), *C. albicans* (Phillips and Balish, 1966; Sundstrom *et al.*, 2002; Mason *et al.*, 2012) and *E. coli* LF82 (Chassaing *et al.*, 2014), but this study was the first to use *R. intestinalis* and our strain of *R. gnavus*. In addition, this is the first time,

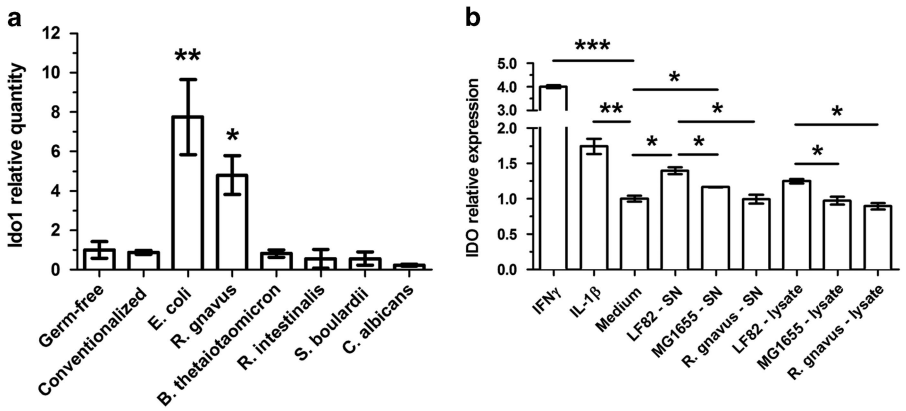

Figure 8 *E. coli* LF82 induces IDO expression in colon epithelial cells. To confirm microarrays, the expression of IDO was determined by RT-qPCR in the colon of mono-associated mice (**a**) and in human colon HT-29 cell line with luciferase reporter submitted to *E. coli* strains, our *R. gnavus* strain, or controls (**b**). For RT-qPCR, ΔΔCt quantification method was used, with GAPDH as an internal control and germ-free group as a calibrator. Ido1 relative quantity and IDO relative expression are expressed as mean ± s.e.m. ($n = 3$ or 5 per group). Statistical comparison with the germ-free group or between strains was performed using Mann–Whitney *U*-test (*$P<0.05$/**$P<0.01$/***$P<0.001$). Panel **b** is representative of two independent assays.

Figure 7 *B. thetaiotaomicron* mono-association upregulates Treg pathways. (**a**) Heatmap representing the microarray colon expression of selected genes involved in Treg pathways, when compared with the germ-free group. (**b**) The expression of three major genes involved in Treg pathways was determined in colon by RT-qPCR, using ΔΔCt quantification method with GAPDH as an internal control and germ-free group as a calibrator. (**c**) Colon samples were fixed in paraformaldehyde acid, embedded in paraffin and sliced in 4-µm sections, then stained by immunohistochemistry with rabbit polyclonal anti-Foxp3 antibody (Treg cells). In graphs, results are expressed as mean ± s.e.m. ($n = 5$ per group) and statistical comparison with the germ-free group (panel **b**) or between groups (panel **c**) was performed using Mann–Whitney *U*-test (*$P<0.05$/**$P<0.01$/***$P<0.001$). Representative photos were taken with x100 magnification. Bt, *B. thetaiotaomicron*; Conv, conventionalized; Ec, *E. coli*; GF, germ-free; Rg, *R. gnavus*; Ri, *R. intestinalis*.

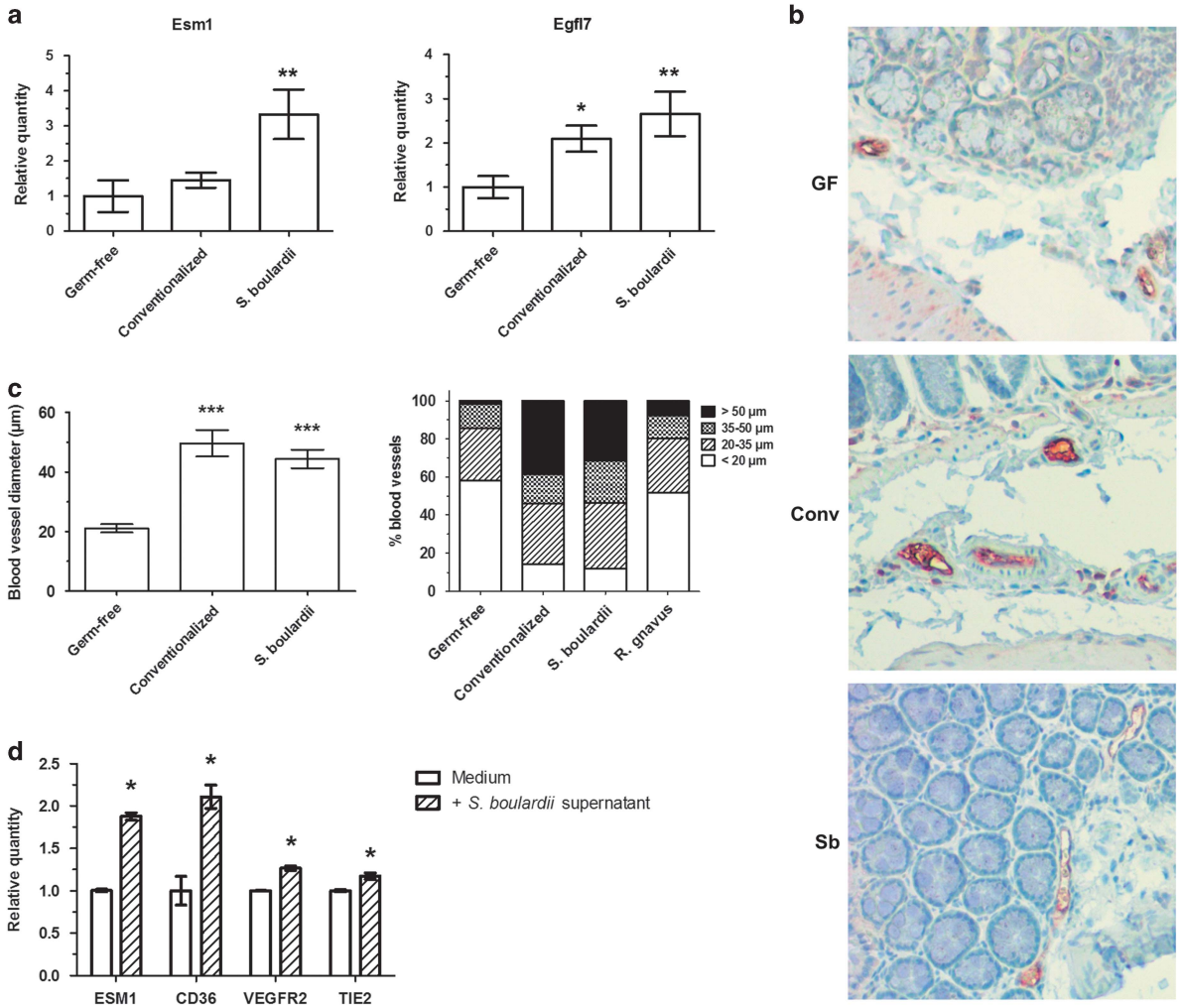

Figure 9 *S. boulardii* modulate angiogenesis and increases blood vessel diameter in colon. (**a**) To confirm microarrays, the expression of two endothelial genes was determined in colon by RT-qPCR, using ΔΔCt quantification method with GAPDH as an internal control and germ-free group as a calibrator. (**b** and **c**) Colon samples were fixed in paraformaldehyde acid, embedded in paraffin and sliced in 4-µm sections, then stained by immunohistochemistry with rabbit polyclonal anti-CD31 antibody (endothelial cells) to determine blood vessel diameter. (**d**) The expression of four endothelial genes was determined in HUVEC cell line with or without *S. boulardii* supernatant by RT-qPCR, using ΔΔCt quantification method with GAPDH as an internal control and medium as a calibrator. In graphs, results are expressed as mean or mean ± s.e.m. ($n = 5$ per group) and statistical comparison with the germ-free group or calibrator was performed using Mann–Whitney *U*-test ($^*P<0.05/^{**}P<0.01/^{***}P<0.001$). Representative photos were taken with x100 magnification. Conv, conventionalized; GF, germ-free; Sb, *S. boulardii*.

to our knowledge that all of these mono-associations were studied together and to such an extent.

First, we observed that the global colonic transcriptional response of mono-colonized mice was much closer to that of the germ-free mice than the conventionalized mice. Nevertheless, some mono-associated models showed very specific and original transcriptomic patterns. The *B. thetaiotaomicron* model was surprisingly and particularly close to conventionalized mice in terms of global transcriptomics and to some extent in immune maturation. The colonization of germ-free mice with this bacterium alone seemed to promote the maturation of the colonic immune system. In comparison with conventionalized mice, it also decreased colon epithelial cell proliferation, as shown in the Ki67 immunochemistry staining and as illustrated by the downregulation of pathways involved in DNA and cell division processes. Notably, the Treg pathways were highly induced by *B. thetaiotaomicron*, with the FoxP3 gene being even more expressed than it was in conventionalized mice. The number of Treg in colon was also increased by the bacterium. Although the exact mechanism must be investigated, this Treg cell induction could be linked to SCFA production by *B. thetaiotaomicron*. In fact, propionate and acetate, which were shown to promote Treg cell expansion directly in the colon (Arpaia *et al*., 2013; Furusawa *et al*., 2013), were found to be significantly increased in the cecum of *B. thetaiotaomicron* mono-colonized mice. Interestingly, other species from the *Bacteroides* genus have been shown to induce Treg cells in the colon. Polysaccharide A from *Bacteroides fragilis* reportedly led the cellular

and physical maturation of the developing immune system (Mazmanian *et al*., 2005), especially with the induction of colon Treg cells to promote immune tolerance (Round *et al*., 2011). As *B. thetaiotaomicron* can also produce polysaccharidic capsules (Burt *et al*., 1978), identifying a polysaccharide A-like molecule and assessing its effects could lead to interesting insights to explain the Treg-associated gene induction by *B. thetaiotaomicron*. Furthermore, the induction or expansion of Treg cells can be induced in mice by altered Schaedler flora that consist of eight species of microbiota dominated by a bacterium related to *Bacteroides distasonis* (Geuking *et al*., 2011). It would therefore be of great interest to confirm the expansion of Treg cells into the colon of *B. thetaiotaomicron* mono-associated mice and to identify the mechanisms involved. *Bacteroides* species may also have pro-inflammatory effects as some of them have been shown to induce colitis in genetically susceptible mice deficient for TGFβ and IL-10 receptors (Bloom *et al*., 2011). Interestingly, these pathways are among the key one involved in Treg cells regulatory effects.

R. gnavus mono-associated mice exhibited a remarkable transcriptomic profile with a top upregulated signature that contained metabolic pathways and was not linked to the immune response when compared with germ-free mice. Notably, *R. gnavus* induced the activation of several genes and pathways involved in tryptophan metabolism. Indeed, tryptophan hydroxylase 1 and IDO expression were induced by *R. gnavus*, and these two enzymes are responsible for tryptophan degradation into 5-hydroxytryptophane (the first step in serotonin and melatonin synthesis) and kynurenine, respectively. Moreover, the melatonin, nicotin and serotonin degradation pathways were activated downstream of these reactions (Figure 3b). As these tryptophan metabolites are involved in neurological and intestinal functions (Chen *et al*., 2011; Yao *et al*., 2011; Anderson *et al*., 2012; Mawe and Hoffman, 2013), the *R. gnavus* effect should be further investigated with respect to these issues.

S. boulardii mono-associated mice also presented a 'non-immune' top upregulated signature when compared with germ-free mice. Vascular genes and functions were particularly regulated by *S. boulardii* and these results were confirmed by colon histology, showing an increased vessel size in comparison with germ-free mice. *S. boulardii* was previously associated with vascular events and angiogenesis. In fact, it reportedly inhibited vascular endothelial growth factor receptor signaling and angiogenesis in intestinal inflammation to limit this inflammation and promote mucosal tissue repair (Chen *et al*., 2013). However, our results significantly differed. Instead of inhibition, *S. boulardii* led to a modulation of angiogenesis and a maturation of blood vessels in our hands, given that we observed the upregulation of genes involved in pro-angiogenic (Esm1, Egfl7, Vegfr2, Tie2) and anti-angiogenic (Col18a1, CD36) pathways, in addition to larger blood vessels without significantly modified numbers. This apparent discrepancy is certainly related to the differences between the selected models. Conventional mice with DSS-induced colitis were used in Chen *et al*., and healthy mono-associated mice were used in our study. In any case, because angiogenesis has a major role in IBD pathogenesis (Hatoum and Binion, 2005; Chidlow *et al*., 2006; Danese *et al*., 2007; Scaldaferri *et al*., 2009), precisely unraveling the mechanisms by which *S. boulardii* modulates endothelial cells and angiogenesis to mature blood vessels may be of great interest. Submitting a *S. boulardii* mono-associated model to colitis and comparing the vascular results with that of colitis in conventional or conventionalized mice could yield important information. Polyamines were reported to modulate angiogenesis (Gao *et al*., 2013; LaRocca *et al*., 2013) and were produced by *S. boulardii* (Buts and De Keyser, 2006,2010), and they could present an interesting direction to follow. Interestingly, although it is also a fungus, *C. albicans* induced very different effects in the host compared with *S. boulardii*. This difference was clear in the transcriptomics results in addition to the colon histology and cytokine production. Notably, the *S. boulardii*-associated transcriptomic profile was intermediate between germ-free and conventionalized mice profiles, whereas the *C. albicans*-associated transcriptomic profile was totally different from that of the control groups. Moreover, the cytokine production pattern in MLNs was dominantly pro-inflammatory with *C. albicans* (with high levels of IFNγ, IL-17 and IL-22), whereas it was mostly anti-inflammatory with *S. boulardii* (with low levels of IFNγ and IL-17). These results are in accordance with the reported effects of *C. albicans* and *S. boulardii* in colitis models, exhibiting pro- and anti-inflammatory properties, respectively (Jawhara and Poulain, 2007; Jawhara *et al*., 2008; Lee *et al*., 2009).

Finally, we showed that *E. coli* LF82 strongly induced IDO gene expression in mice and in human intestinal epithelial cells, in contrast with commensal *E. coli* MG1655. This induction has already been reported for *E. coli* in several cellular models (Loughman and Hunstad, 2011; Kassianos *et al*., 2012; Loughman and Hunstad, 2012), but this is the first time that it was found in colon cells and for the LF82 strain. IDO gene induction may be caused by *E. coli*-induced type I and type II IFN responses because these cytokines are potent inducers of IDO (Dai and Gupta, 1990a,b) or may be a direct effect of the bacterium. With regards to the indirect effect of *E. coli* through IFNγ, we showed that *E. coli* LF82 highly induced IFNγ gene expression in mice (Figure 4), and intestinal epithelial cells do not express IDO at steady state (Choudhry *et al*., 2009a,b; Ogawa *et al*., 2012). However, we showed that *E. coli* LF82 induced IDO in the colon epithelial cell line independently from IFNγ, which was also reported for uropathogenic *E. coli* in bladder epithelial cells

(Loughman and Hunstad, 2012). In addition, the same study also reported that commensal non-pathogenic *E. coli* did not induce IDO upregulation. Therefore, a direct induction of IDO by *E. coli* LF82 seems to be most likely. As IDO presents immunomodulatory effects (Mellor and Munn, 2004), we can hypothesize that the bacterium set up this mechanism to protect itself from the immune response. In fact, this strategy is used by other pathogens (Boasso, 2011; de Souza Sales *et al*., 2011; Makala *et al*., 2011). Another possibility would be that *E. coli* LF82 uses the anti-infectious effects of IDO activation via tryptophan starvation (Pfefferkorn, 1984; Byrne *et al*., 1986; Zelante *et al*., 2009) to keep other competitors away from its niche. In any case, further tests are needed to understand this IDO induction by *E. coli* LF82.

Thus, the microorganisms we studied have very different effects on host. Based on the genome-wide transcriptomics data in mono-colonized mice, we notably pointed out and confirmed some specific effects such as Treg induction or angiogenesis. Although the monoxenic models we used are artificial and the obtained results could be different in a complex microbiota context, our results suggest that, beside global and possibly nonspecific effects of the microbiota on host, some microorganisms may have more specific effects with limited redundancy within the microbiota. These effects may be strain or species specific or even conserved at the genus level. However, a common perturbation in the number or activity of a microbial population involved in one of these specific effects could have major effects on host physiology. This may be the case in the numerous human disease associated with dysbiosis.

In conclusion, although our study have been performed in monoxenic models that are physiologically very different from a complex microbiota context, it revealed that microorganisms with a potential role in intestinal homeostasis and inflammation may have specific impacts on the host, highlighting the complexity of microbiota–host interactions. Gut microbiota and most of the studied microorganisms had major effects on immune functions. Among them, *B. thetaiotaomicron* had the most impressive effect, being almost able to recapitulate the effects of the whole microbiota. In addition, we noted the effects of *E. coli* AIEC LF82 on IDO activation and of *S. boulardii* CNCM I-745 on angiogenesis modulation and the maturation of blood vessels. Our results also suggest that *R. gnavus* has major effects on metabolism. Interestingly, microorganisms known to be increased in IBD patients' microbiota (*E. coli* AIEC LF82, *R. gnavus* and *C. albicans*) exhibited a mostly pro-inflammatory pattern, whereas those known to be decreased or potentially protective in IBD (*R. intestinalis*, *S. boulardii)* exhibited a mostly anti-inflammatory pattern. Beyond the information on the role of each microorganism, this work proposes several new directions to better understand IBD pathogenesis and identify therapeutic targets.

Conflict of Interest

The authors declare no conflict of interest.

Acknowledgements

This study was funded by Biocodex Laboratories, and TWH received a grant from Biocodex Laboratories to complete this work. BL and HS received financial support from the ATIP-AVENIR program. We thank the members of the ANAXEM germ-free platform for their valued assistance in mouse care, in addition to J Lecardonnel from the CRB GADIE core facility (INRA, Jouy en Josas, France) for his technical assistance and expertize in microarrays. We also thank the Centre de Recherche en Nutrition Humaine (Nantes), especially V Ferchaud-Roucher, for the SCFA quantification.

References

Anderson G, Maes M, Berk M. (2012). Inflammation-related disorders in the tryptophan catabolite pathway in depression and somatization. *Adv Protein Chem Struct Biol* **88**: 27–48.

Arpaia N, Campbell C, Fan X, Dikiy S, van der Veeken J, deRoos P *et al.* (2013). Metabolites produced by commensal bacteria promote peripheral regulatory T-cell generation. *Nature* **504**: 451–455.

Bloom SM, Bijanki VN, Nava GM, Sun L, Malvin NP, Donermeyer DL *et al.* (2011). Commensal bacteroides species induce colitis in host-genotype-specific fashion in a mouse model of inflammatory bowel disease. *Cell Host Microbe* **9**: 390–403.

Boasso A. (2011). Wounding the immune system with its own blade: HIV-induced tryptophan catabolism and pathogenesis. *Curr Med Chem* **18**: 2247–2256.

Boudeau J, Glasser AL, Masseret E, Joly B, Darfeuille-Michaud A. (1999). Invasive ability of an *Escherichia coli* strain isolated from the ileal mucosa of a patient with Crohn's disease. *Infect Immun* **67**: 4499–4509.

Burt S, Meldrum S, Woods DR, Jones DT. (1978). Colonial variation, capsule formation, and bacteriophage resistance in Bacteroides thetaiotaomicron. *Appl Environ Microbiol* **35**: 439–443.

Buts JP, De Keyser N. (2006). Effects of *Saccharomyces boulardii* on intestinal mucosa. *Dig Dis Sci* **51**: 1485–1492.

Buts JP, De Keyser N. (2010). Transduction pathways regulating the trophic effects of *Saccharomyces boulardii* in rat intestinal mucosa. *Scand J Gastroenterol* **45**: 175–185.

Byrne GI, Lehmann LK, Landry GJ. (1986). Induction of tryptophan catabolism is the mechanism for gamma-interferon-mediated inhibition of intracellular *Chlamydia psittaci* replication in T24 cells. *Infect Immun* **53**: 347–351.

Carvalho FA, Barnich N, Sauvanet P, Darcha C, Gelot A, Darfeuille-Michaud A. (2008). Crohn's disease-associated *Escherichia coli* LF82 aggravates colitis in

injured mouse colon via signaling by flagellin. *Inflamm Bowel Dis* **14**: 1051–1060.
Cascone T, Heymach JV. (2012). Targeting the angiopoietin/Tie2 pathway: cutting tumor vessels with a double-edged sword? *J Clin Oncol* **30**: 441–444.
Chassaing B, Koren O, Carvalho FA, Ley RE, Gewirtz AT. (2014). AIEC pathobiont instigates chronic colitis in susceptible hosts by altering microbiota composition. *Gut* **63**: 1069–1080.
Chen CQ, Fichna J, Bashashati M, Li YY, Storr M. (2011). Distribution, function and physiological role of melatonin in the lower gut. *World J Gastroenterol* **17**: 3888–3898.
Chen X, Yang G, Song JH, Xu H, Li D, Goldsmith J *et al.* (2013). Probiotic yeast inhibits VEGFR signaling and angiogenesis in intestinal inflammation. *PLoS One* **8**: e64227.
Chidlow Jr JH, Langston W, Greer JJ, Ostanin D, Abdelbaqi M, Houghton J *et al.* (2006). Differential angiogenic regulation of experimental colitis. *Am J Pathol* **169**: 2014–2030.
Choudhry N, Korbel DS, Edwards LA, Bajaj-Elliott M, McDonald V. (2009a). Dysregulation of interferon-gamma-mediated signalling pathway in intestinal epithelial cells by *Cryptosporidium parvum* infection. *Cell Microbiol* **11**: 1354–1364.
Choudhry N, Korbel DS, Zaalouk TK, Blanshard C, Bajaj-Elliott M, McDonald V. (2009b). Interferon-gamma-mediated activation of enterocytes in immunological control of Encephalitozoon intestinalis infection. *Parasite Immunol* **31**: 2–9.
Dai W, Gupta SL. (1990a). Molecular cloning, sequencing and expression of human interferon-gamma-inducible indoleamine 2,3-dioxygenase cDNA. *Biochem Biophys Res Commun* **168**: 1–8.
Dai W, Gupta SL. (1990b). Regulation of indoleamine 2,3-dioxygenase gene expression in human fibroblasts by interferon-gamma. Upstream control region discriminates between interferon-gamma and interferon-alpha. *J Biol Chem* **265**: 19871–19877.
Danese S, Sans M, Spencer DM, Beck I, Donate F, Plunkett ML *et al.* (2007). Angiogenesis blockade as a new therapeutic approach to experimental colitis. *Gut* **56**: 855–862.
Darfeuille-Michaud A, Neut C, Barnich N, Lederman E, Di Martino P, Desreumaux P *et al.* (1998). Presence of adherent Escherichia coli strains in ileal mucosa of patients with Crohn's disease. *Gastroenterology* **115**: 1405–1413.
Darfeuille-Michaud A, Boudeau J, Bulois P, Neut C, Glasser AL, Barnich N *et al.* (2004). High prevalence of adherent-invasive Escherichia coli associated with ileal mucosa in Crohn's disease. *Gastroenterology* **127**: 412–421.
de Souza Sales J, Lara FA, Amadeu TP, de Oliveira Fulco T, da Costa Nery JA, Sampaio EP *et al.* (2011). The role of indoleamine 2, 3-dioxygenase in lepromatous leprosy immunosuppression. *Clin Exp Immunol* **165**: 251–263.
Febbraio M, Hajjar DP, Silverstein RL. (2001). CD36: a class B scavenger receptor involved in angiogenesis, atherosclerosis, inflammation, and lipid metabolism. *J Clin Invest* **108**: 785–791.
Ferchaud-Roucher V, Pouteau E, Piloquet H, Zair Y, Krempf M. (2005). Colonic fermentation from lactulose inhibits lipolysis in overweight subjects. *Am J Physiol Endocrinol Metab* **289**: E716–E720.
Furusawa Y, Obata Y, Fukuda S, Endo TA, Nakato G, Takahashi D *et al.* (2013). Commensal microbe-derived butyrate induces the differentiation of colonic regulatory T cells. *Nature* **504**: 446–450.
Gao JH, Guo LJ, Huang ZY, Rao JN, Tang CW. (2013). Roles of cellular polyamines in mucosal healing in the gastrointestinal tract. *J Physiol Pharmacol* **64**: 681–693.
Geuking MB, Cahenzli J, Lawson MA, Ng DC, Slack E, Hapfelmeier S *et al.* (2011). Intestinal bacterial colonization induces mutualistic regulatory T cell responses. *Immunity* **34**: 794–806.
Giaffer MH, Holdsworth CD, Duerden BI. (1991). The assessment of faecal flora in patients with inflammatory bowel disease by a simplified bacteriological technique. *J Med Microbiol* **35**: 238–243.
Giaffer MH, Holdsworth CD, Duerden BI. (1992). Virulence properties of *Escherichia coli* strains isolated from patients with inflammatory bowel disease. *Gut* **33**: 646–650.
Hatoum OA, Binion DG. (2005). The vasculature and inflammatory bowel disease: contribution to pathogenesis and clinical pathology. *Inflamm Bowel Dis* **11**: 304–313.
Hooper LV, Wong MH, Thelin A, Hansson L, Falk PG, Gordon JI. (2001). Molecular analysis of commensal host-microbial relationships in the intestine. *Science* **291**: 881–884.
Humbert L, Maubert MA, Wolf C, Duboc H, Mahe M, Farabos D *et al.* (2012). Bile acid profiling in human biological samples: comparison of extraction procedures and application to normal and cholestatic patients. *J Chromatogr B Analyt Technol Biomed Life Sci* **899**: 135–145.
Jawhara S, Poulain D. (2007). *Saccharomyces boulardii* decreases inflammation and intestinal colonization by *Candida albicans* in a mouse model of chemically-induced colitis. *Med Mycol* **45**: 691–700.
Jawhara S, Thuru X, Standaert-Vitse A, Jouault T, Mordon S, Sendid B *et al.* (2008). Colonization of mice by *Candida albicans* is promoted by chemically induced colitis and augments inflammatory responses through galectin-3. *J Infect Dis* **197**: 972–980.
Joossens M, Huys G, Cnockaert M, De Preter V, Verbeke K, Rutgeerts P *et al.* (2011). Dysbiosis of the faecal microbiota in patients with Crohn's disease and their unaffected relatives. *Gut* **60**: 631–637.
Kassianos AJ, Hardy MY, Ju X, Vijayan D, Ding Y, Vulink AJ *et al.* (2012). Human CD1c (BDCA-1)+ myeloid dendritic cells secrete IL-10 and display an immuno-regulatory phenotype and function in response to *Escherichia coli*. *Eur J Immunol* **42**: 1512–1522.
Khor B, Gardet A, Xavier RJ. (2011). Genetics and pathogenesis of inflammatory bowel disease. *Nature* **474**: 307–317.
Kirchhelle A, Fruhwein N, Toburen D. (1996). [Treatment of persistent diarrhea with *S. boulardii* in returning travelers. Results of a prospective study]. *Fortschr Med* **114**: 136–140.
LaRocca TJ, Gioscia-Ryan RA, Hearon CM Jr, Seals DR. (2013). The autophagy enhancer spermidine reverses arterial aging. *Mech Ageing Dev* **134**: 314–320.
Lecuit M, Sonnenburg JL, Cossart P, Gordon JI. (2007). Functional genomic studies of the intestinal response to a foodborne enteropathogen in a humanized

gnotobiotic mouse model. *J Biol Chem* **282**: 15065–15072.

Lee SK, Kim YW, Chi SG, Joo YS, Kim HJ. (2009). The effect of *Saccharomyces boulardii* on human colon cells and inflammation in rats with trinitrobenzene sulfonic acid-induced colitis. *Dig Dis Sci* **54**: 255–263.

Ley RE, Peterson DA, Gordon JI. (2006). Ecological and evolutionary forces shaping microbial diversity in the human intestine. *Cell* **124**: 837–848.

Loughman JA, Hunstad DA. (2011). Attenuation of human neutrophil migration and function by uropathogenic bacteria. *Microbes Infect* **13**: 555–565.

Loughman JA, Hunstad DA. (2012). Induction of indoleamine 2,3-dioxygenase by uropathogenic bacteria attenuates innate responses to epithelial infection. *J Infect Dis* **205**: 1830–1839.

Makala LH, Baban B, Lemos H, El-Awady AR, Chandler PR, Hou DY *et al.* (2011). Leishmania major attenuates host immunity by stimulating local indoleamine 2,3-dioxygenase expression. *J Infect Dis* **203**: 715–725.

Mangin I, Bonnet R, Seksik P, Rigottier-Gois L, Sutren M, Bouhnik Y *et al.* (2004). Molecular inventory of faecal microflora in patients with Crohn's disease. *FEMS Microbiol Ecol* **50**: 25–36.

Martins FS, Silva AA, Vieira AT, Barbosa FH, Arantes RM, Teixeira MM *et al.* (2009). Comparative study of *Bifidobacterium animalis, Escherichia coli, Lactobacillus casei* and *Saccharomyces boulardii* probiotic properties. *Arch Microbiol* **191**: 623–630.

Mason KL, Erb Downward JR, Mason KD, Falkowski NR, Eaton KA, Kao JY *et al.* (2012). *Candida albicans* and bacterial microbiota interactions in the cecum during recolonization following broad-spectrum antibiotic therapy. *Infect Immun* **80**: 3371–3380.

Mawe GM, Hoffman JM. (2013). Serotonin signalling in the gut–functions, dysfunctions and therapeutic targets. *Nat Rev Gastroenterol Hepatol* **10**: 473–486.

Maynard CL, Elson CO, Hatton RD, Weaver CT. (2012). Reciprocal interactions of the intestinal microbiota and immune system. *Nature* **489**: 231–241.

Mazmanian SK, Liu CH, Tzianabos AO, Kasper DL. (2005). An immunomodulatory molecule of symbiotic bacteria directs maturation of the host immune system. *Cell* **122**: 107–118.

McFarland LV, Surawicz CM, Greenberg RN, Fekety R, Elmer GW, Moyer KA *et al.* (1994) A randomized placebo-controlled trial of *Saccharomyces boulardii* in combination with standard antibiotics for Clostridium difficile disease. *JAMA* **271**: 1913–1918.

Mellor AL, Munn DH. (2004). IDO expression by dendritic cells: tolerance and tryptophan catabolism. *Nat Rev Immunol* **4**: 762–774.

Nichol D, Stuhlmann H. (2012). EGFL7: a unique angiogenic signaling factor in vascular development and disease. *Blood* **119**: 1345–1352.

Ogawa K, Hara T, Shimizu M, Nagano J, Ohno T, Hoshi M *et al.* (2012). (-)-Epigallocatechin gallate inhibits the expression of indoleamine 2,3-dioxygenase in human colorectal cancer cells. *Oncol Lett* **4**: 546–550.

Perez-Munoz ME, Bergstrom K, Peng V, Schmaltz R, Jimenez-Cardona R, Marsteller N *et al.* (2014). Discordance between changes in the gut microbiota and pathogenicity in a mouse model of spontaneous colitis. *Gut Microbes* **5**: 286–295.

Pfefferkorn ER. (1984). Interferon gamma blocks the growth of *Toxoplasma gondii* in human fibroblasts by inducing the host cells to degrade tryptophan. *Proc Natl Acad Sci USA* **81**: 908–912.

Phillips AW, Balish E. (1966). Growth and invasiveness of *Candida albicans* in the germ-free and conventional mouse after oral challenge. *Appl Microbiol* **14**: 737–741.

Pothoulakis C. (2009). Review article: anti-inflammatory mechanisms of action of *Saccharomyces boulardii. Aliment Pharmacol Ther* **30**: 826–833.

Qin J, Li R, Raes J, Arumugam M, Burgdorf KS, Manichanh C *et al.* (2010). A human gut microbial gene catalogue established by metagenomic sequencing. *Nature* **464**: 59–65.

Richard ML, Lamas B, Liguori G, Hoffmann TW, Sokol H. (2015). The gut fungal microbiota: the Yin and Yang of inflammatory bowel disease. *Inflamm Bowel* **21**: 656–665.

Rocha SF, Schiller M, Jing D, Li H, Butz S, Vestweber D *et al.* (2014). Esm1 modulates endothelial tip cell behavior and vascular permeability by enhancing VEGF bioavailability. *Circ Res* **115**: 581–590.

Rodrigues AC, Nardi RM, Bambirra EA, Vieira EC, Nicoli JR. (1996). Effect of *Saccharomyces boulardii* against experimental oral infection with *Salmonella typhimurium* and *Shigella flexneri* in conventional and gnotobiotic mice. *J Appl Bacteriol* **81**: 251–256.

Roskoski Jr R. (2008). VEGF receptor protein-tyrosine kinases: structure and regulation. *Biochem Biophys Res Commun* **375**: 287–291.

Round JL, Lee SM, Li J, Tran G, Jabri B, Chatila TA *et al.* (2011). The Toll-like receptor 2 pathway establishes colonization by a commensal of the human microbiota. *Science* **332**: 974–977.

Scaldaferri F, Vetrano S, Sans M, Arena V, Straface G, Stigliano E *et al.* (2009). VEGF-A links angiogenesis and inflammation in inflammatory bowel disease pathogenesis. *Gastroenterology* **136**: 585–595 e585.

Seksik P, Rigottier-Gois L, Gramet G, Sutren M, Pochart P, Marteau P *et al.* (2003). Alterations of the dominant faecal bacterial groups in patients with Crohn's disease of the colon. *Gut* **52**: 237–242.

Sokol H, Lay C, Seksik P, Tannock GW. (2008a). Analysis of bacterial bowel communities of IBD patients: what has it revealed? *Inflamm Bowel Dis* **14**: 858–867.

Sokol H, Pigneur B, Watterlot L, Lakhdari O, Bermudez-Humaran LG, Gratadoux JJ *et al.* (2008b). *Faecalibacterium prausnitzii* is an anti-inflammatory commensal bacterium identified by gut microbiota analysis of Crohn disease patients. *Proc Natl Acad Sci USA* **105**: 16731–16736.

Standaert-Vitse A, Sendid B, Joossens M, Francois N, Vandewalle-El Khoury P, Branche J *et al.* (2009). *Candida albicans* colonization and ASCA in familial Crohn's disease. *Am J Gastroenterol* **104**: 1745–1753.

Sundstrom P, Balish E, Allen CM. (2002). Essential role of the *Candida albicans* transglutaminase substrate, hyphal wall protein 1, in lethal oroesophageal candidiasis in immunodeficient mice. *J Infect Dis* **185**: 521–530.

Willing BP, Dicksved J, Halfvarson J, Andersson AF, Lucio M, Zheng Z *et al.* (2010). A pyrosequencing study in twins shows that gastrointestinal microbial profiles vary with inflammatory bowel disease phenotypes. *Gastroenterology* **139**: 1844–1854 e1841.

Wrzosek L, Miquel S, Noordine ML, Bouet S, Joncquel Chevalier-Curt M, Robert V *et al.* (2013). Bacteroides

thetaiotaomicron and *Faecalibacterium prausnitzii* influence the production of mucus glycans and the development of goblet cells in the colonic epithelium of a gnotobiotic model rodent. *BMC Biol* **11**: 61.

Yao K, Fang J, Yin YL, Feng ZM, Tang ZR, Wu G. (2011). Tryptophan metabolism in animals: important roles in nutrition and health. *Front Biosci (Schol Ed)* **3**: 286–297.

Zelante T, Fallarino F, Bistoni F, Puccetti P, Romani L. (2009). Indoleamine 2,3-dioxygenase in infection: the paradox of an evasive strategy that benefits the host. *Microbes Infect* **11**: 133–141.

Supplementary Information accompanies this paper on The ISME Journal website (http://www.nature.com/ismej)